

CONTROL OF POROUS STRUCTURE OF PAPER IN A CONTINUOUS PROCESS

Christian Mair

KTH – Royal Institute of Technology, Stockholm, Sweden
Delfort, Wattens, Austria
email: christianmair@delfortgroup.com

ABSTRACT

Microfibrillated cellulose (MFC) has unique properties which can lead to interesting new paper applications. Some applications strongly rely on defined paper pore structures, like filter paper for water purification or separator paper in batteries. The pore structure modification of a paper sheet through MFC is investigated. The combination of MFC and polyelectrolytes (PEs) enables a pore dimension reduction of an existing softwood base layer. In both handsheet and pilot paper machine trials this effect was accomplished and reproducible. It was shown that MFC grammage, MFC consistency and PE type are significant factors that affect the pore dimension.

1 INTRODUCTION

The growing market opportunities through novel nanomaterials, like cellulose nanofibres and microfibrillated cellulose, enable the development of new production methods and innovative products to sustain competitive power within the industry. Currently the use of cellulose nanomaterial in papermaking aims mostly towards the improvement of mechanical and barrier properties to increase filler content and decrease oxygen permeability, respectively [1, 2]. However, the possibilities with cellulose nanomaterials are exceeding the mentioned applications. Extraordinary properties of cellulosic nanomaterials enable advanced

applications as several research papers have shown, e.g. electrode material for batteries, gas diffusion layers in fuel cells or membranes for water purification [3–6]. Taking these unconventional applications as an example it becomes clear that a continuous production method with full control of the pore structure is essential for their market success. Therefore the primary objectives for this project are, first, to introduce cellulose nanomaterial into a papermaking process to understand and identify dominant mechanisms concerning retention, dewatering and formation of nanocellulose paper sheets, and second to controllably modify paper surface properties through a continuous papermaking process with the help of cellulose nanomaterials. The results will offer basic understanding for applications like water purification or separators for electrochemical energy devices where precise surface properties are crucial for the products' purpose, i.e. pore size dimensions are limited. Hence, pore size and pore size distribution (PSD) will be critical parameters to characterise progress towards the goal of the project.

2 THEORY

The structure of paper is of utmost importance as it influences most of the physical properties, e.g. porosity. The porosity of a sheet is given by the fraction of the void volume in relation to the entire sheet volume. Hence dimensions of fibres and filler particles control porosity [7]. In this project no filler is used wherefore the porosity is fully determined by presence and absence of cellulosic material. The higher the porosity value the more void volume exists in the sheet with expected typical ranges from 0.3 to 0.7 [8, 9]. In foresight to filter or separator applications it is beneficial to aim for higher porosity values as a lower pressure drop or better electrolyte wettability is expected, respectively. According to studies from Maki more void space correlates with larger pore radii and higher air permeability [10]. The author confirmed different effects of fibre types, beating degrees and calendaring on paper properties, especially pore dimensions. With conventional processing methods (i.e. beating) the dimensions and stiffness of fibres can be reduced so that the fibres are shortened and collapse. The average pore radii of paper made from beaten, unbleached kraft fibres range from *ca.* 0.5 μm (84° SR) to *ca.* 1.5 μm (24° SR) [11]. However, intensive beating up to 84° SR is energy- and time-consuming, which limits the control of the pore dimensions by mechanical treatment in refiners.

With increasing porosity also the number of pores per area rises [7]. Niskanen found that the number of pores per area depends on the flexibility and the thickness-to-width ratio of fibres. As short fibres are stiffer than long fibres it can be concluded that hardwood sheets have more pores per area [12]. However, more

pores do not automatically lead to a higher air permeability. Since the pore radii are smaller for hardwood handsheets the air permeability is usually lower using this fibre type [10]. For this reason softwood (SW) sheets are considered in this project as the air permeability is higher and it is easier to detect significant variations.

The inter-fibre pore size is affected by the basis weight and thickness of the sheet. Measurements done by Corte show that the pore radii are inversely related to the sheet's basis weight [8]. Recent investigations verified this effect and predicted the mean pore dimension of a paper sheet. The extensive work from Sampson and Urquhart presented a theory for the distribution of the narrowest dimension of pores encountered in a path through a fibre network. The mean pore dimension is inversely proportional to the areal density of the network, proportional to a simple function of porosity and influenced also by fibre dimensions [13].

As a consequence the proposed method in this study is to change the dimension of the fibre drastically to sub-micrometre range while aiming for a low sheet grammage. In the literature it is reported that smaller fibre dimensions are able to establish smaller mean in plane pore dimensions [7, 13–15], therefore the use of nanocellulosic material can be beneficial to achieve this goal.

3 EXPERIMENTAL

To achieve control over the porous paper structure an unconventional approach is selected. The beginning state is defined by a specified SW base sheet. This sheet is made from refined and unrefined SW fibres and represents the reference pore size distribution. Through modifications with MFC and PEs the pore dimensions will be reduced as the final results show. Basically the cross-sectional arrangement will be two-layered with a mechanical support layer at the bottom (SW) and a selective top layer (MFC + PE). Both laboratory and pilot-scale trials will be performed to prove that pore dimensions can be adapted by the supportive use of MFC and PE.

3.1 Materials

MFC material with the market name Exilva was provided by Borregaard (Sarpsborg, Norway). Two types were investigated, characterised by low and high fibrillation degree (type P and F, respectively). The MFC is available in gel and paste form, whereas only the paste form was used. In **Table 1** the investigated MFC and PE types are listed including their main physical and chemical properties. Cationic PE were provided by BASF (Ludwigshafen, Germany) – polyethylenimine (PEI),

Table 1. Properties of MFC and PEs; HS – used for handshets, Pilot – used for pilot trial

<i>MFC type</i>	<i>DC</i> [wt%]	<i>Aggregate size</i> [μm]	<i>Viscosity</i> [cP]	<i>Anionic surface charge</i> [$\mu\text{eq/g}$]
P (HS)	10.2	56	19000	25.82 \pm 0.68
F (HS)	9.5	32	22000	22.98 \pm 0.65
P (Pilot)	10.6	60	20000	–
<i>PE name</i>	<i>Type</i>	<i>Z-average</i> [nm]	<i>Cationic surface charge</i> [$\mu\text{eq/g}$]	
Polymin SK	PEI ¹	486.8 \pm 78.7	5797 @ pH 5.56	
Polymin VT	PVAm ¹	24.6 \pm 0.2	1347 @ pH 5.31	
Polymin VZ	PVAm ²	23.2 \pm 0.7	629 @ pH 5.55	
Percol 8400X	PAM ^{1,3}	695.8 \pm 13.9	2780 @ pH 6.41	
Percol 8397X	PAM ^{1,4}	194.5 \pm 23.0	–	

¹ High MW, ² Med MW, ³ High CD, ⁴ Low CD (according to supplier), MW – molecular weight, CD – charge density

polyvinyl amine (PVAm) and polyacrylamide (PAM). Northern bleached SW kraft (Södra green 85FZ – dry content (DC) 93.90 wt%) was purchased from Södra Cell (Mönsterås, Sweden).

3.2 Methods

3.2.1 Characterisation of MFC and PE

The data characterizing the MFC was provided by the supplier. Aggregate size was determined through static light scattering with the Microtrac S3500 from an aqueous MFC suspension. The Brookfield viscosity was measured at 2 wt% DC and V-73 spindle (10 rpm, 5 min).

Type and approximate molecular weight range of the PE was provided by the supplier. The cationic PE as well as the anionic MFC surface charge was measured with the Microtrac Stabino Particle Charge Titration Analyzer diluted with MilliQ water. The Z-average is the intensity weighted mean hydrodynamic size of particles measured by dynamic light scattering with the Malvern Instruments Zetasizer Nano ZS.

3.2.2 Handsheet preparation

The base sheet for handsheet forming was produced on the pilot paper machine (PM). The sheets were made of 70 parts initial SW and 30 parts beaten SW for 45 min in a valley beater at 1.57% consistency. Targeted grammage was 30 gsm under defined process conditions. The base sheet reel was cut in squares of known

area (approx. 30×30 cm) and the exact grammage was noted for determination of MFC add-on. The weighted base paper was placed on the pre-wetted wire of the Frank-PTI Rapid Köthen Sheet Machine Automatic and the forming cylinder was closed. The MFC paste was dispersed in deionized water using an IKA T 25 digital Ultra-Turrax disperser. Dispersion was done at 10000 rpm for 4 min at 0.1% consistency. Optional PE were added to the MFC suspension under manual stirring with a glass rod 1 min before application onto the base layer. Then the MFC suspension with 0.01% consistency was gently poured into the forming cylinder to merge with the base layer. After dewatering, a blotting paper was superposed to the wet sheet and compressed using a 3 kg roll (four passes). Drying was carried out under vacuum (-950 mbar) between two blotting papers at 90 °C for 10 min. After drying a circular piece (1 dm²) was punched out and weighed in order to calculate the applied amount of MFC by subtracting the actual base sheet grammage noted before.

3.2.3 Pilot paper machine production

The pilot PM consists of two 400 litre (base layer) and two 300 litre (top layer) storage tanks for disintegrated pulp suspensions and one 800 litre tank for the circulation system. Through speed controlled screw pumps the suspensions are transported at defined volume flows to two radial distributors. This is also the injection point for additional PE that are pumped into the system by a dosage pump. The radial distributors are connected to one of the headbox layers where the suspension impinges on the inclined wire (30° inclination). The wire has a width of 30 cm and first passes along a suction box and then three additional suction lines. The forming section is controlled by the lid opening of the corresponding headbox layer (exit flow velocity), the valve opening for the suction devices and further the wire speed. Manometers connected to each suction device measure the dewatering pressure. The white water from the suction box is pumped through another screw pump to the circulation tank. This water acts as dilution water of the thick stock coming from the pulp storage tank and is mixed with the thick stock prior to the first radial distributor.

After forming the paper is transferred to the press felt to reach the first press. The nip pressure can be set from 0 to 4 bar. The final stage is the drying section where the paper is placed on the drying felt. The felt conveys the paper around the steam drying cylinder which can reach up to 100 °C.

The stratified headbox enables simultaneous formation of a two layered web. The bottom layer is a 30 gsm SW kraft mixture (see section 3.2.2) and the top layer consists of MFC with adjustable grammage (0.1% and 0.02% consistency, respectively). Disintegration of the cellulose material was done in a pilot pulper at 2.5% consistency, 1500 rpm, 10 min (SW) and 0.5% consistency, 2500 rpm,

15 min (MFC) entirely in tap water. For the whole papermaking process tap water is used. The production speed was set to 2 m/min to ensure sufficient dewatering at the suction spots along the wire. The press was set to 2 bar nip pressure and the drying cylinder was heated to 95 °C.

3.2.4 Paper measurements

Sheets were equilibrated in a conditioned environment at 23 °C and 50% relative humidity for 24 hours. Air permeability was determined according to ISO 2965 at fifteen different positions per paper sample (Borgwaldt A10). A pressure gradient of 1 kPa is applied across the sheet and the volumetric flow of air per area is measured, given in ml/cm²/min. Gas diffusion capacity was determined according to CORESTA Recommended Method N° 77 (Borgwaldt A50). A concentration gradient across the sheet between 0 (pure N₂) and 100% CO₂ allows the measurement of diffused CO₂ through the paper, given in cm/s. Tensile strength was measured following the TAPPI T494 standard (L&W Tensile Tester). Sample stripes, 15 mm wide and 100 mm long, were analysed, results given in N/15 mm. Paper thickness was analysed in accordance with TAPPI T411. Capillary flow porosimetry (CFP) was the analytical method to measure the porous paper structure. The analysis was done with the Quantachrome Porometer 3Gzh and Porofil as wetting liquid following the ASTM Method F316. SEM pictures were taken with the JEOL NeoScope JCM-5000 where no further sample preparation was done.

4 RESULTS

4.1 Handsheets

To evaluate the interaction of SW base layer, MFC and PE two layered handsheets were produced. Pre-trials with 7.5 gsm and 15 gsm MFC on the 30 gsm SW base sheet showed an exceptionally fast dewatering behaviour using the F type MFC. The dewatering time was reduced from 955 ± 53 s (P type MFC) to 383 ± 15 s (F type MFC) when 15 gsm MFC was added without PEs. Calculating the retention showed only 53.1 wt% of F type stayed on the sheet, while 87.5 wt% of P type was retained. The beneficial retention characteristics of the P type lead to further investigations of this MFC type only. The exceptionally high MFC grammage prohibited a successful CFP measurement. The high MFC grammage reduced porosity and air permeability drastically which consequently lead to insufficient gas flow through the CFP specimen and no measurement results could be obtained.

Consequently the MFC grammage was limited to 2.5 gsm and 5 gsm in order to have a sufficiently porous structure to study the physical paper properties. The radar chart in **Figure 1** (left) shows decreasing air permeability and diffusion capacity for all samples compared to the reference without MFC. At 5 gsm MFC the air permeability is ca. 5 ml/min/cm², whereas 10 to 100 times higher values are noted for 2.5 gsm. A consistency increase from 0.01% to 0.1% leads to higher air permeability and diffusion capacity levels. The combination of MFC and PE shows significant effects on the paper properties in contrast to handsheets with MFC only. Polymin VT has an air permeability limiting effect, whereas Percol 8397X shows an enhancing effect. Tensile strength, however, increases for all samples as MFC is added. The most significant increase occurs with 5 gsm MFC.

Further analysis by CFP shows the actual pore dimensions of the handsheet samples (see **Table 2**). Base. 2 is the base layer with the highest air permeability and has the highest mean pore diameter (pore diameter at 50% cumulative flow through the sample). Modification of the base layer through MFC addition reduces the pore diameter. This effect is enhanced when PE are added. Polymin VT shows the lowest air permeability as well as the smallest mean pore diameter. In contrast MFC addition at 0.1% consistency leads to the largest pore dimensions among MFC modified handsheets. The addition of 5 gsm MFC reduces the air flow through the sample thus prohibiting an effective analysis by the porosimeter.

Percol 8397X and 8400X provide paper sheets with larger pore dimensions. The base layer for these two handsheets was from a different production and showed different air permeability (Base.2).

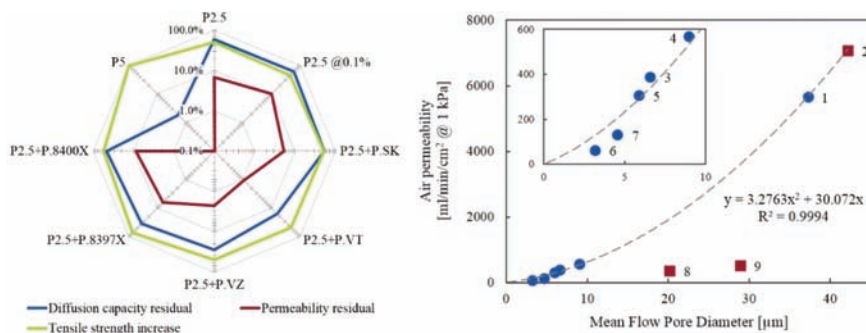


Figure 1. (Left) Logarithmic radar chart with handsheet properties. ‘Residual/increase’ defines remaining/gaining percentage compared to base layer without MFC. P2.5 describes 2.5 gsm MFC add-on at 0.01% consistency (unless noted). Additional labels are PE types at 127 mg PE/g dry MFC. (Right) Correlation between air permeability and mean flow pore diameter with data points from Table 2. Handsheets with Base.1 (blue circles), with Base.2 (red squares).

Table 2. Analytical summary from CFP for handsheets with 2.5 gsm MFC add-on and PE addition

Sample	Pore diameter [μm]		Air permeability	
	min	mean	max	[ml/min/cm ² @ 1 kPa]
Base.1 ¹	35.5	37.5	51.0	5650.0± 477.0
Base.2 ^{2,2}	35.2	42.2	66.1	7061.0±1521.0
P2.5 ³	5.6	6.6	15.4	386.4± 39.1
P2.5@0.1% ⁴	6.9	9.0	16.0	567.4± 69.4
P.SK ⁵	3.7	5.9	12.8	303.3± 37.2
P.VT ⁶	2.3	3.2	20.6	60.5±10.0
P.VZ ⁷	2.6	4.6	32.1	129.3± 4.5
P.8397X ⁸	14.1	20.2	30.3	355.4± 30.1
P.8400X ⁹	25.3	28.9	31.2	507.4± 56.6

^a Base layer for P.8397X and 8400X

¹⁻⁹ Data point description in **Figure 1** (*right*)

Figure 1 (*right*) displays the 2nd order polynomial regression line of air permeability versus the mean flow pore diameter. As the pore diameter gets smaller the air permeability decreases quadratically. The R-squared value of 0.9994 shows a good correlation of the data points. Handsheets with Percol 8397X and 8400X (red squares), however, show no correlation with the other samples.

Figure 2 illustrates the complete PSD obtained by CFP. The y-axis in the diagram shows the differential pore flow that expresses the percentage of the total gas flow through pores with a given diameter. The solid and dotted blue line (Base.1 and Base.2, respectively) represent both base layer without MFC addition, therefore showing the largest mean pore diameter. Applying MFC with and without PE shifts the PSD towards smaller pore dimensions. Polymin VT and VZ provide the broadest PSDs and at the same time the smallest pore dimensions.

The influence of PE concentration on the handsheet air permeability was tested. Polymin SK added to MFC suspension with concentrations ranging from 2–127 mg PE/g dry MFC showed a decrease in air permeability at increasing PE concentrations. The air permeability stagnates for concentrations above 10 mg PE/g dry MFC. This behaviour validates comparable effects for Polymin SK concentrations alternating from 10–127 mg PE/g dry MFC.

4.2 Pilot paper machine

With handsheet pre-trials the most suitable MFC (P type MFC), its optimum grammage (2.5 gsm) and a supportive PE (Polymin SK, 10 mg/g dry MFC) was

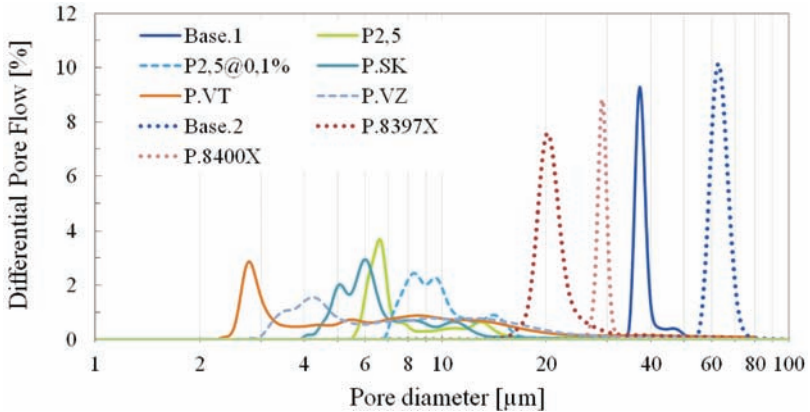


Figure 2. PSD with logarithmic scaling on x-axis showing samples from Table 2.

determined. The MFC type and the PE concentration was kept constant in the pilot scale trials. Process parameters were optimised to match the handsheet properties, i.e. the consistency of base and MFC layer, lip height for each headbox layer to achieve controlled flow velocities, dewatering settings and the grammage for the MFC layer. **Figure 3 (left)** shows the influence of increasing MFC grammage on the resulting pore diameter. The addition of 11 gsm MFC leads to a similar PSD as for a handsheet with 2.5 gsm MFC and Polymin VT. The retention at pilot scale is lower than in the lab environment, wherefore a higher amount of initial MFC is used to achieve comparable results.

Figure 3 (right) shows the negative dewatering pressure on individual dewatering spots along the wire during forming. The base layer is easy to dewater, while additional MFC increases the dewatering resistance. The green curve indicates a steady state operation and was achieved by running a single paper quality with constant parameters until the stock containers were empty. Here 7 gsm MFC were added to confirm the reproducibility of the results.

Figure 4 displays several SEM images that show the base layer and its partial coverage by MFC through the optimal grammage and PE addition.

5 DISCUSSION

As “nanocellulosic material” covers a broad spectrum of materials it is necessary to know the characteristics of the used material. The MFC can be seen as a coherent 3D network of fibrils and bundles of fibrils in the micrometre range,

where single fibrils have diameters in the nanometre range (10 nm–100 nm) and bundles thereof in the lower micrometre range. Through the different production methods P type and F type have different aggregate sizes. The more intense treatment of F type MFC might lead to a bigger fraction of non-coherent fibrils in nanometre size. Consequently this non-coherent fraction together with the smaller aggregate size explains the lower retention of F type MFC in handsheet trials.

The application of MFC increases the tensile strength of the sheet as seen in **Figure 1 (left)**. The higher tensile strength values are presumably due to the fact that MFC is more fibrillated and has more degrees of freedom than the external fibrils on the base layer fibre created by refining [16]. The increased number of hydrogen bonds eventually leads to higher tensile strength values [17]. Interestingly the different MFC and PE types do not have significant influence on the tensile strength, it rather depends on the MFC grammage applied to the base layer.

Air permeability properties are influenced by MFC and PE. The correlation of air permeability and mean pore flow diameter in **Figure 1 (right)** is a guidance for pilot scale trials. It confirms that air permeability can be a reliable predictor of the pore dimensions of a paper sheet. However, as the base layer is produced on the pilot PM process variations can occur which cause the different properties of Base.1 and Base.2. Both base layers are positioned on the regression line which would imply that the modification by MFC should be the same for both. CFP results verify that the mean pore flow diameter of Base.2 is larger than of Base.1. The MFC mean aggregate size is 56 μm , hence it is less likely for MFC aggregates/flocs to span over pore openings that exceed their own size. The probability for the aggregate to pass through the sheet or partly cover a pore is higher for Base.2 than for Base.1 [18]. Therefore the pore dimensions for handsheets made with Percol 8397X and Percol 8400X are larger than MFC modified handsheets made with Base.1.

From these results it can be concluded that the modification of the base layer pore structure is very particular. MFC and PEs can be utilised to alter a specific base layer with defined properties. For base layers with different pore dimensions MFC grammage and PE concentrations need to be adjusted.

Change of MFC consistency during handsheet forming had a significant influence on the sheet properties. The different consistency results in a change of the crowding number which defines the number of contacts a fibre undergoes in a given spherical volume. As the consistency increases, the crowding number does too. Hence, the mean number of MFC aggregates in a suspension (or any given spherical volume) increases and flocculation of MFC is more likely [19]. The anionic character of MFC can form a loosely packed agglomeration due to the electrostatic repulsion of the charged groups. The floc size may further be associated with the creation of lower density areas between the flocs which then result

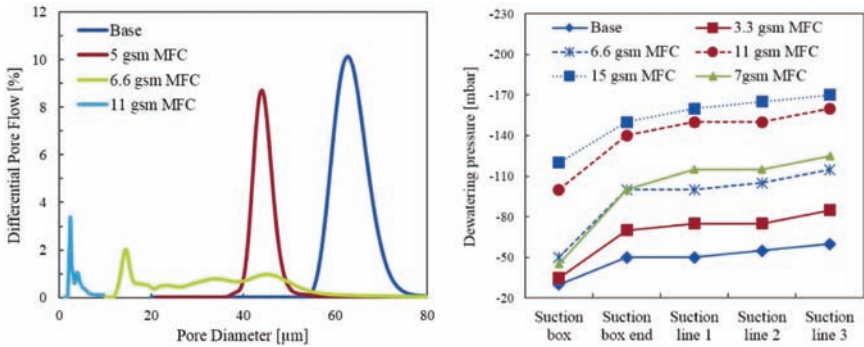


Figure 3. (Left) PSD of pilot PM paper samples. (Right) Dewatering pressure along the suction spots along the wire.

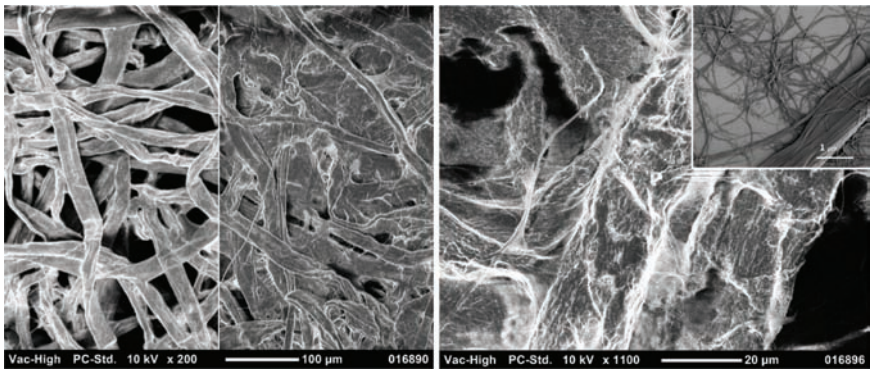


Figure 4. (Left) SEM of unmodified base layer (left-side) and additional 11 gsm MFC produced in pilot scale (right-side): (Right) SEM of handsheet with 2.5 gsm MFC and 10 mg Polymin VT/g MFC, (top-right corner) SEM of MFC aggregate [21].

in bigger pore dimensions [20]. This can be an explanation why the handsheet with 0.1% MFC consistency has larger pore dimensions than the handsheet with 0.01% MFC consistency.

Besides beating and calendaring the main parameter to control paper pore dimension is grammage. The inverse relation of grammage and pore radii documented in literature can be reproduced with the recent results [8, 11]. High SW fibre grammage leads to several theoretical single layers above each other and the probability for pores to be connected from top to bottom is reduced [12, 15]. The same could be claimed for MFC, however, its minuscule dimensions do not allow a formation as it is expected for SW fibres. Handsheets with 15 gsm, 7.5 gsm or

5 gsm MFC seem to establish a coherent film on the base layer surface. With decreasing MFC grammage and consequently MFC film surface coverage the pore dimensions must move towards the pore dimension of the base layer. Hence, applying 2.5 gsm MFC is an acceptable grammage that works with the defined SW layer.

Mixing the MFC with PE reduces the pore dimensions in comparison with reference handsheets (2.5 gsm MFC only). The measurement of the paper parameters reveals the differences of the utilised PE types. The modification was also detected by CFP as the pore dimensions were altered. The minimum and mean pore diameter were the smallest when using Polymin VT, followed by Polymin VZ and Polymin SK. Usually PE are used as retention and flocculation aids, hence they promote flocculation of MFC aggregates [20]. Despite increased floc size the pore dimensions were reduced compared to the reference handsheet as shown by the PSD. Cationic PE lead to higher viscosity of MFC suspensions under shear flow [22], thus it might be concluded that PE have a bridging effect between anionic MFC aggregates. The PE help to form a denser and bigger floc which is held together by electrostatic forces. Consequently, these flocs can span over a larger distance from the pore's edge and narrow the pore dimension. This effect can be seen in **Figure 4 (right)** where the left top corner shows a MFC film that spans from the edge of the pore towards its centre and thus reducing the pore dimension. However, the right bottom corner reveals an open pore that is not affected by the MFC. The restriction of the base layer pore dimension is observably controlled by this effect.

The pore dimensions of paper sheets with Polymin VT and Polymin VZ show a rather broad distribution compared to the other samples (**Figure 3**). Due to their low air permeability the sample diameter was increased from 25 mm to 47 mm. Process variations during papermaking can cause the formation of pinholes which result in exceptionally big pores. Even after the addition of MFC some of the pinholes keep their full diameter. During CFP pinholes are more likely detected when analysing samples with a large diameter, which broadens the PSD.

PAM with low cationic surface charge (Percol 8397X) tends to show a PSD with smaller pore dimensions than their highly surface charged counterpart. However, for PVAm the high surface charged type (Polymin VT) reveals smaller pore dimensions. Looking at the polymer chain length high MW PVAm leads to smaller pore dimensions than the medium MW PVAm (Polymin VZ). In case of PAM both types have high MW. The low surface charged PE can establish a less compressed conformation on the MFC surface, while high surface charged PE create a relatively flat conformation [23]. This could give an indication on how the charge density controls the pore dimension. Yet, it seems difficult to draw conclusions on its influence from the given data. The significant influence on pore

dimensions from the PE perspective comes primarily from the utilised type and then its individual properties.

Figure 3 (*left*) shows the outcomes obtained by increasing MFC grammage on the pilot PM. As the MFC grammage increases the pores get gradually constricted wherefore the detected pore dimension decreases. The concurrent forming of both layers through the stratified headbox decreases the first pass retention of MFC. During pilot forming the base layer is not fully formed when the MFC approaches the base. Therefore MFC flocs will penetrate the base sheet whereas MFC stayed on the base layer surface in handsheet trials. The SEM image (**Figure 4**, *left*) shows some distinct SW fibres on the surface which confirms the diffuse border between top and base layer. To achieve the same pore-restricting effect the MFC grammage is increased in pilot trials. Improvements in first-pass MFC retention were achieved when the flow velocities of the two layers started to match. However, due to equipment limitations a full alignment was not possible.

The individual dewatering pressure progressions in **Figure 3** (*right*) show trends towards certain pore dimensions. As the dewatering pressure increases the pore dimensions decrease since more MFC aggregates are captured inside initial pores [18]. A repeated trial with a fixed amount of 7 gsm MFC replicates the previous results and confirms the reproducibility of the paper manufactured on the pilot PM.

6 CONCLUSION

This work has shown that the addition of microfibrillated cellulose and polyelectrolytes are effective in altering the pore structure of existing paper sheets. Findings from initial trials in laboratory scale were successfully implemented on pilot scale. These findings involve the optimal MFC type, MFC grammage, PE type (PEI, PVAm and PAM) and its concentration. With appropriate choice of MFC and PE and their parameters it is well viable to adjust the pore dimensions of a defined SW base sheet. The MFC/PE-interaction will influence the resulting MFC flocs which eventually constrain the pore structure. Handsheet trials confirm 2.5 gsm MFC as sufficient grammage to have a significant effect on the pore dimension. However, samples produced on the pilot PM needed 7 gsm MFC to show a similar effect in comparison to the handsheets. Addition of polymers further promotes decrease and control of the pore dimensions. The exact dimensions will be ultimately controlled both by MFC grammage and PE type. It is possible to keep the pore size in a controllable range between 1.8 μm to 4.8 μm with 11 gsm MFC and 10 mg PEI per g dry MFC.

REFERENCES

1. M. Ankerfors, T. Lindström and D. Söderberg, “The use of microfibrillated cellulose in fine paper manufacturing – Results from a pilot scale papermaking trial,” *Nord. Pulp Pap. Res. J.*, **29**(3): 476–483, 2014.
2. N. Lavoine, I. Desloges, B. Khelifi and J. Bras, “Impact of different coating processes of microfibrillated cellulose on the mechanical and barrier properties of paper,” *J. Mater. Sci.*, **49**(7): 2879–2893, 2014.
3. D. Beneventi, D. Chaussy, D. Curtil, L. Zolin, E. Bruno, R. Bongiovanni, M. Destro, C. Gerbaldi, N. Penazzi and S. Tapin-Lingua, “Pilot-scale elaboration of graphite/microfibrillated cellulose anodes for Li-ion batteries by spray deposition on a forming paper sheet,” *Chem. Eng. J.*, **243**: 372–379, 2014.
4. L. Zolin, M. Destro, D. Chaussy, N. Penazzi, C. Gerbaldi and D. Beneventi, “Aqueous processing of paper separators by filtration dewatering: towards Li-ion paper batteries,” *J. Mater. Chem. A*, **3**(28): 14894–14901, 2015.
5. L. Isikel, I. Gocek and S. Adanur, “Design and characterization of nonwoven fabrics for gas diffusion layer in polymer electrolyte membrane fuel cell,” *J. Text. Inst.*, **101**(11): 1006–1014, Nov. 2010.
6. H. Ma, C. Burger, B. S. Hsiao and B. Chu, “Ultra-fine cellulose nanofibers: new nano-scale materials for water purification,” *J. Mater. Chem.*, **21**(21): 7507, 2011.
7. K. Niskanen, “Paper Physics,” in *Papermaking Science and Technology*, H. Paulapuro (Ed.), Helsinki: Fapet Oy, 2008.
8. H. Corte, “The Porosity of Paper,” in *Handbook of Paper Science, Volume 2, The Structure and Physical Properties of Paper*, H. F. Rance (Ed.), Wiltshire: Elsevier Scientific Publishing, 1982, 1–70.
9. W. W. Sampson, “Materials properties of paper as influenced by its fibrous architecture,” *Int. Mater. Rev.*, **54**(3):, 134–156, May 2009.
10. S. Maki, “State of Pores in Paper and Physical Properties of Paper,” 2010.
11. H. Corte, “The porous structure of paper: Its measurement, its importance and its modification by beating,” in *Fundamentals of Papermaking Fibres*, Vol 1., F. Bolam (Ed.), London: British Paper and Board Makers Assn., 1958, 301–331.
12. R. C. Neagu, “Stiffness contribution of various wood fibers to composite materials,” *J. Compos. Mater.*, **40**(8): 663–699, 2005.
13. W. W. Sampson and S. J. Urquhart, “The contribution of out-of-plane pore dimensions to the pore size distribution of paper and stochastic fibrous materials,” *J. Porous Mater.*, **15**(4): 411–417, Aug. 2008.
14. M. Rasi, *Permeability Properties of Paper*, University of Jyväskylä, 2013.
15. D. Li, M. W. Frey and Y. L. Joo, “Characterization of nanofibrous membranes with capillary flow porometry,” *J. Memb. Sci.*, **286**(1–2): 104–114, 2006.
16. T. Taipale, M. Österberg, A. Nykänen, J. Ruokolainen and J. Laine, “Effect of microfibrillated cellulose and fines on the drainage of kraft pulp suspension and paper strength,” *Cellulose*, **17**(5): 1005–1020, 2010.
17. K. Sim Hye Jung Youn, “Preparation of porous sheets with high mechanical strength by the addition of cellulose nanofibrils,” *Cellulose*, **23**(2): 1383–1392, 2016.

18. K. Athley, L. Granlöf, D. Söderberg, M. Ankerfors and G. Ström, “Mechanical retention – Influence of filler floc size and grammage of the fibre web,” *Nord. Pulp Pap. Res. J.*, **27**(2): 202–207, Jun. 2012.
19. M. Alava and K. Niskanen, “The physics of paper,” *Reports Prog. Phys.*, **69**(3): 669–723, 2006.
20. S. Varanasi and W. Batchelor, “Superior non-woven sheet forming characteristics of low-density cationic polymer-cellulose nanofibre colloids,” *Cellulose*, **21**(5): 3541–3550, 2014.
21. A. Karppinen, “Microfibrillated cellulose or nanocellulose,” 2016. [Online]. Available: <http://blog.exilva.com/microfibrillated-cellulose-or-nanocellulose> [accessed: 8th October 2016].
22. A. Karppinen, A. H. Vesterinen, T. Saarinen, P. Pietikäinen and J. Seppälä, “Effect of cationic polymethacrylates on the rheology and flocculation of microfibrillated cellulose,” *Cellulose*, **18**(6): 1381–1390, 2011.
23. J. C. Roberts, *The Chemistry of Paper*, The Royal Society of Chemistry, 1996.

Transcription of Discussion

CONTROL OF POROUS STRUCTURE OF PAPER IN A CONTINUOUS PROCESS

Christian Mair

KTH Royal Institute of Technology, Stockholm, Sweden; and Delfort,
Wattens, Austria

Thierry Mayade Ahlstrom-Munksjö Apprieu

Could you convince us, or at least me, that with more conventional paper making techniques, like selecting of other fibres, playing with the refining, we cannot get the same result as the one you got with the routine MFCs, which are not so easy to get and difficult to process?

Christian Mair KTH Royal Institute of Technology

Probably, I will have a hard time to convince you, but for me this was my Master's thesis, I was interested in pilot scale forming and also the MFC as a new type of material, and I tried to look for a different way of how to use this material instead of just increasing the strength properties of paper or even increasing the filler content while maintaining strength properties. Even with some future work and optimization of the base sheet by refining and by selecting the right pulp fibre type, then at some point you will get to a natural limit. However, by using new type of fibres, like MFC, NFC with their miniscule dimensions; you might even get better results, I could imagine.

Bill Sampson University of Manchester

I think the real issue here is the difference between what the distribution is and what you are measuring. At the start of your talk, you correctly stated that you can change the apparent pore size, by changing grammage, in fact you don't change

Discussion

pore size by changing grammage, but you change the measurement because fluid porometry, which you have been using, measures the narrowest path. So what you have done is put a film on top of a base sheet; it wouldn't matter what the base sheet was, you are measuring the properties of just the MFC film. This is why, as you put more MFC down, you see a narrowing of the measured pore size, whereas the pore size in the MFC film is actually the same. You see a very broad pore size distribution from one of your films and that is almost certainly the film is being damaged by the process of measuring. It is really very important to look at what the measurement process is. We know from 50 years of theoretical work looking at what you can achieve with fibrous objects (regardless of whether they are nanofibres, microfibrils or infinite lines) that it is very hard to stop the pore size distribution exhibiting a gamma or a log normal distribution. So when you see the type of very broad distribution you are seeing, you know that something different is happening. This was first observed by Heinz Corte in the 1950s, where it was pin holes being put into the sheet; you are doing the same here. In your case, the pin holes aren't the pin holes from the base paper. They are almost certainly holes being made in your film by the process of measuring.

Christian Mair

Thank you. I didn't really go into the measurement analysis, it was done externally, so I had to accept the results as they were and they seemed plausible to me, but after your explanations continuing the work on this topic should be considered.

Gil Garnier Monash University

Very nice work, Christian. Did you compare the polyelectrolyte addition only to the MFC fraction that is then mixed with the fibres furnish versus polyelectrolyte addition to the whole mixture of fibres on the paper machine, and if so what conclusions did you find or what did you expect?

Christian Mair

Polyelectrolytes were only added to MFC to induce flocculation, but not to the whole mixture. It was always just a two-layered approach, so the whole mixture with MFC fibres and the polyelectrolytes was not planned to be formed at once.

Gil Garnier

Second question: when you moved from the hand sheet to the continuous machine, did you find that the best polymer or that the optimum dosage varied?

Christian Mair

When I went to the pilot scale, I decided on one polyelectrolyte type, which was polyethyleneimine.

Gil Garnier

Was the best optimum polymer dosage on the machine the same as on the hand sheet?

Christian Mair

Yes, that was the same, 10 mg per gram of dry MFC.

Wolfgang Bauer Graz University of Technology

Did you also compare your results to coating an MFC film on top of the base sheet?

Christian Mair

I did not have the opportunity to apply a film on the base sheet. Probably the hand sheet forming acted like adding a film because the retention was almost at 100%, the conditions were controlled so I could retain almost all of the MFC on the hand sheet. This can be compared to a film, but then again I have no SEM pictures and no actual data to say if this is true.